NACA

RESEARCH MEMORANDUM

DESIGN AND EXPERIMENTAL INVESTIGATION OF A SINGLE-STAGE TURBINE WITH A ROTOR ENTERING RELATIVE MACH NUMBER OF 2

By Thomas P. Moffitt

Lewis Flight Propulsion Laboratory
Cleveland, Ohio

NATIONAL ADVISORY COMMITTEE
FOR AERONAUTICS

WASHINGTON

September 15, 1958

NATIONAL ADVISORY COMMITTEE FOR AERONAUTICS

RESEARCH MEMORANDUM

DESIGN AND EXPERIMENTAL INVESTIGATION OF A SINGLE-STAGE TURBINE WITH A ROTOR ENTERING RELATIVE MACH NUMBER OF 2*

By Thomas P. Moffitt

SUMMARY

The design and experimental investigation of a single-stage supersonic turbine are presented herein. The turbine was designed for a rotor entering relative Mach number of 2.

The maximum equivalent specific work output of the turbine at design speed and approximately design over-all pressure ratio was 32.9 Btu per pound at a static efficiency of 0.414. This static efficiency gave good verification to an independent reference that indicated theoretical static efficiencies for similar single-stage turbines within the range 0.40 to 0.45.

An experimental ratio of effective rotor blade momentum thickness to mean camber length was determined to be 0.0114, which compares favorably with the results obtained from several transonic and subsonic turbines. The design procedure for this turbine would have been improved by allowing for more rotor losses by assuming a value of this momentum parameter comparable with those obtained from transonic turbines.

Removing a large portion of the rotor suction surface enabled a lower static pressure to be felt at the stator exit at the expense of higher rotor losses. The net result was an improvement in turbine work output of about 3 percent at design setting conditions.

No problems associated with supersonic starting were encountered even under the worst conditions of turbine operation with respect to this problem.

INTRODUCTION

In recent years there has been an increasing interest in turbines applicable to rocket-pump drive. In view of this, a considerable amount of the turbine research effort at the NACA Lewis laboratory has been

* Title, Unclassified.

directed toward turbines suitable for this purpose. Because a rocket must carry all the fuel and oxidant required for propulsion, including the turbopump driving fluid, problems associated with total gross weight are necessarily encountered. From a weight standpoint, two of the desirable characteristics of a turbine designed for rocket-pump application are to use a minimum amount of driving fluid and to be light weight.

One type of turbine that appears attractive for this application would be a supersonic turbine utilizing a high pressure drop across a minimum number of stages. Such a turbine would be light weight and have rotor blades designed for a high turning angle that would result in a high specific work output per stage. For a given power application, then, this type of turbine would require only a small amount of working fluid to drive it. The expected efficiency from such a turbine would be considerably lower than that of more conservative turbines because of higher leaving losses. However, the desirable characteristics of being a simple, lightweight, high specific work output, low mass flow turbine might easily outweigh the disadvantage of a low efficiency.

Very little information is available regarding the performance of supersonic turbines. Cascade results of stator blade rows and rotor blade rows are available (e.g., refs. 1 and 2), but a need exists for information concerning the performance of the two operating together as a turbine unit. The purpose of this investigation, then, is to gain a better understanding of the general performance characteristics of supersonic turbines.

A single-stage turbine with a rotor entering relative Mach number of 2 was designed, constructed, and experimentally investigated at the Lewis laboratory. In addition to the instrumentation required to determine over-all turbine performance, static-pressure taps were provided in the outer housing across the blade rows in an effort to gain an understanding of the major trends encountered within the flow passages as the turbine went through off-design conditions of operation.

The performance of the turbine in terms of static efficiency is compared with the results of reference 3, which includes theoretical static efficiencies of single-stage turbines with similar design characteristics.

SYMBOLS

c_p specific heat at constant pressure, Btu/lb-$^\circ$F

D blade surface diffusion parameter, $1 - \frac{\text{Velocity after diffusion}}{\text{Velocity before diffusion}}$

$\Delta h'$ specific work output, Btu/lb

l length of blade mean camber line, ft

M Mach number

p pressure, lb/sq ft

T temperature, $^{\circ}F$

U blade speed, ft/sec

V absolute gas velocity, ft/sec

w weight-flow rate, lb/sec

z stator stacking point

γ ratio of specific heats

δ ratio of inlet air total pressure to NACA standard sea-level pressure, p_0'/p^*

ε function of γ, $\frac{\gamma^*}{\gamma}\left[\frac{\left(\frac{\gamma+1}{2}\right)^{\frac{\gamma}{\gamma-1}}}{\left(\frac{\gamma^*+1}{2}\right)^{\frac{\gamma^*}{\gamma^*-1}}}\right]$

η_s static efficiency, based on static- to total-pressure ratio across turbine, p_4/p_0'

θ_{cr} squared ratio of critical velocity at turbine inlet to critical velocity at NACA standard sea-level temperature, $(V_{cr,0}/V_{cr}^*)^2$

$\overline{\theta}$ effective rotor blade momentum thickness based on turbine over-all performance, ft

Subscripts:

cr conditions at Mach number of 1.0

m mean section

R relative to rotor blade

s	static-pressure-tap measuring station
tot	sum of suction- and pressure-surface quantities
x	axial component
0	turbine inlet
1	stator exit before mixing
2	stator exit after mixing, also rotor inlet
3	rotor exit before mixing
4	rotor exit after mixing, also turbine outlet

Superscripts:

'	absolute total state
*	NACA standard conditions

TURBINE DESIGN

General Design Characteristics

The single-stage turbine investigated had a 10.3-inch mean diameter with a hub-tip radius ratio of 0.9 at the rotor inlet with the blade heights increased to a hub-tip radius ratio of 0.87 at the rotor outlet. The turbine was designed for a rotor entering relative Mach number of 2.0.

The design equivalent parameters selected are as follows:

Specific work, $\Delta h'/\theta_{cr}$, Btu/lb 39.0

Weight flow, $\frac{w\sqrt{\theta_{cr}}}{\delta}\varepsilon$, lb/sec 0.585

Mean blade speed, $U_m/\sqrt{\theta_{cr}}$, ft/sec 342

General Design Procedure

All the calculations used in determining the design velocity diagrams, stator blade shape, and rotor blade shape were based on conditions at the mean blade radius. It was assumed that no significant change in flow characteristics would occur radially because of the high hub-tip radius ratio which resulted in blade heights of approximately 1/2 inch.

Velocity diagrams. - The after-mixing velocity diagrams together with a sketch of a typical blade channel showing the station nomenclature used are shown in figure 1. The stator and rotor blade configurations were designed to match these after-mixing conditions.

Stator design. - The stator was designed as three sections: a converging section that turned the flow and accelerated the gas from a Mach number of 0.28 at the stator entrance to sonic conditions at the throat, a diverging section that accelerated the flow from sonic at the throat to a Mach number of 2.54 at the exit of the guided channel, and a straight suction surface from the exit of the guided channel downstream to the blade trailing edge. The calculated losses decreased the free-stream Mach number from 2.54 at the stator exit (station 1, fig. 1) to an after-mixing Mach number of 2.43 (station 2, fig. 1).

The converging free-stream section was designed by use of the stream-filament technique as described in reference 4. All the turning of the free-stream flow (72.6°) was accomplished in this section.

The method used in designing the sharp-cornered diverging free-stream section to accelerate the flow from the throat to the exit of the guided channel was the same as that described in reference 1. This type of design represents the shortest possible expansion passage capable of yielding a uniform, shock-free, parallel, exit flow. The resulting variation in design blade surface velocities is shown in figure 2 as a function of percent axial chord.

Boundary-layer growth along the suction surface, pressure surface, and end walls was calculated on the basis of 32 blades by the method developed in reference 5. The boundary-layer growth was then added to the respective free-stream surfaces and end walls and resulted in the final stator blade shape.

Table I shows the coordinates of the mean section template used in the fabrication process. The aluminum blades were made up of radial elements in order to keep the throat openings as close to rectangular as possible.

Calculations based on the design procedure resulted in a 14-percent drop in total pressure across the stator blade row.

Rotor design. - The free-stream rotor passage was designed using the supersonic-vortex-flow theory as described in reference 6. The passage consisted of three sections: an entering transition section where the velocity increased on the suction surface and decreased on the pressure surface; a circular arc section where the velocity remained constant on each respective surface; and an exit transition section where the velocity increased on the pressure surface, and, in this case, remained constant on

the suction surface. The design variation in blade surface relative Mach numbers is shown in figure 2 as a function of percent axial chord. Boundary-layer growth was calculated on the basis of 48 blades and was added to the free-stream surfaces in the same manner as was used in the stator design.

Table II shows the rotor blade coordinates used in the fabrication process. The same coordinates were used for the hub, mean, and tip sections, which allowed the blades to be machined from a continuous piece of aluminum stock. Running clearance between the rotor blades and the outer housing was provided for by cutting a recess in the outer housing (inset, fig. 3) rather than cutting off the outer tips of the rotor blades. The effect of this sharp break is discussed in the section entitled Outer-Wall Static-Pressure Variation.

Calculations based on the design procedure resulted in an expected turbine over-all static efficiency η_s of 0.504 at an over-all static-to total-pressure ratio p_4/p_0' of 0.0333. This efficiency appears high when compared with that which could be expected from the results of reference 3. This reference indicates theoretical static efficiencies in the neighborhood of from 0.40 to 0.45 for a single-stage turbine under similar design conditions.

APPARATUS

The experimental investigation of the turbine was conducted in the same turbine test facility used in reference 7. The apparatus consisted primarily of the turbine configuration, suitable housing to give uniform turbine-inlet flow conditions, and a cradled dynamometer to absorb turbine power output. A diagrammatic sketch of the turbine test section is shown in figure 3. Photographs of the stator and rotor blade configurations are shown in figure 4. The sharp-cornered stator throat openings can be noted from this figure.

The turbine was operated with dry pressurized air from the laboratory combustion-air system. The air passed through a filter tank, heaters, a hydraulically operated inlet control valve, and an ASME flat-plate orifice, and then went to the turbine-inlet air collector. After the air passed through the turbine, it was directed to the laboratory altitude exhaust system.

INSTRUMENTATION

Instrumentation was provided on the turbine apparatus to obtain over-all turbine performance and outer-wall static-pressure variation across the stator and rotor blade rows.

Over-All Turbine Performance

The actual specific work output was computed from weight-flow, torque, and speed measurements. The air weight flow was measured from the calibrated ASME orifice. The turbine output torque was measured with a commercial self-balancing torque cell and mercury manometer. Turbine rotative speed was measured with an electronic events-per-unit-time meter.

Turbine-inlet measurements were taken in the annulus upstream of the stator inlet (station 0, fig. 3). Four static-pressure taps were installed on each of the inner and outer walls and placed on four radial lines 90° apart. Two thermocouple rakes with two bare-wire thermocouples placed at centers of equal annular areas and two total-pressure probes alined axially were mounted in the same plane as the static taps.

Turbine-outlet static pressures were measured in the annulus downstream of the rotor outlet (station 4, fig. 3) from four static-pressure taps spaced 90° apart on each of the inner and outer walls.

Outer-Wall Static-Pressure Variation

A sketch of the location of the static-pressure taps used to measure the outer-wall variation in static pressure across the stator and rotor blade rows is shown in figure 5. Five static-pressure taps were equally spaced in the center of the stator passage from a position just downstream of the stator throat to a position just inside the stator-exit plane. An axial line of 11 equally spaced static-pressure taps was placed across the rotor-inlet and -exit planes as indicated by the figure.

EXPERIMENTAL PROCEDURE

The experimental investigation was conducted by operating the turbine at constant nominal inlet conditions of 75 pounds per square inch absolute and 340° F and at constant speeds of 20, 40, 60, 80, and 100 percent of design speed. For each speed investigated, a range of static- to total-pressure ratios across the turbine p_4/p_0 was set from approximately 0.5 to the minimum that could be obtained, which was about 0.030.

RESULTS AND DISCUSSION

Over-All Turbine Performance

Weight flow. - The investigation was conducted with a weight flow 3.4 percent less than design. The flow remained constant throughout the

entire investigation because sonic conditions were established at the stator throat at an over-all static- to total-pressure ratio across the turbine p_4/p_0' greater than the maximum used to obtain data. This reduction in weight flow was accepted primarily because it represented a discrepancy in stator-throat opening, which was specified as being 0.109 inch, of only 0.003 inch per blade passage. This is within the accuracy of adjustment.

Turbine work output and static efficiency. - The over-all performance of the turbine is presented in figure 6. The equivalent specific work output is shown as a function of over-all pressure ratio for selected values of percent design speed. A grid of static efficiency is also shown on the figure and results directly from the ordinate and abscissa parameters selected and the use of the following expression:

$$\eta_s = \frac{\frac{\Delta h'}{\theta_{cr}}}{c_p T'^* \left[1 - \left(\frac{p_4}{p_0'}\right)^{\frac{\gamma-1}{\gamma}}\right]}$$

The maximum work output was 32.9 Btu per pound and occurred at design speed and approximately design pressure ratio. This represents a maximum work output at design conditions 15.6 percent less than the design value of 39.0 Btu per pound. The static efficiency at this condition was 0.414, which is 9 points below the design value of 0.504. This wide discrepancy is believed to have resulted from calculated losses in the rotor during the design procedure that were considerably smaller than indicated by the experimental investigation. This will be discussed in a subsequent portion of this report.

Figure 6 indicates a sharp break in the operating curve of each speed selected. Because the trend is the same for all speeds, the remainder of the discussion will be limited to design-speed considerations only, since the same discussion would apply to any speed. It is noted that as the exit pressure p_4 is decreased the slope of the work output curve increases with a corresponding increase in both work and efficiency until the sharp break in the curve is reached. At this condition the minimum static pressure and the maximum whirl that could be established at the stator exit have been reached. This minimum stator-exit pressure is limited by the flow conditions within the rotor passage. As the turbine-exit pressure is decreased further, the work output continues to increase but at a slower rate because of an increase in only the rotor-exit whirl, with the stator-exit whirl remaining constant.

Comparison with theoretical results. - As discussed previously, the theoretical results of reference 3 indicate that static efficiencies within the range 0.40 to 0.45 should be expected from single-stage turbines with operating characteristics similar to this turbine. This range compares favorably with the obtained efficiency of 0.414.

The design-point efficiency of 0.504 for this turbine resulted from losses associated with calculated boundary-layer growth. The boundary-layer equations used may or may not have been valid in determining the growth in boundary layer along the blade surfaces. This was not determined. However, an efficiency based on total losses resulting from their use does not appear satisfactory for a turbine of this type.

No distinction was made between the stator and the rotor insofar as boundary-layer equations were concerned. However, reference 3 indicates that rotor loss coefficients twice as great as stator loss coefficients are more reasonable in determining turbine losses. Therefore, it is felt that a larger area allowance should have been made in the design of the rotor blades to account for these higher losses. For the same over-all pressure ratio this would, in effect, decrease both the design-point work and design-point efficiency to more realistic values. In view of the close agreement between the experimental and theoretical values of efficiency, the design procedure would have been improved by assuming a static efficiency based on the theoretical results of reference 3.

Outer-Wall Static-Pressure Variation

Experimental results. - The variation in outer-wall static pressure across the turbine is presented in figure 7(a). The ratio of static pressure at any station to the turbine-inlet total pressure is shown as a function of outer-wall static-pressure-tap measuring stations for various over-all pressure ratios set at design speed. The static-pressure-tap measuring stations indicated correspond to those shown in figure 5.

Figure 7(a) shows that impulse conditions exist across the rotors as the exit pressure is decreased from an over-all pressure ratio of 0.511 to 0.198. During this off-design condition it can be seen from the static-pressure variation of figure 7(a) that a system of oblique shocks passed downstream through the diverging portion of the stator passage with an increase in both stator- and rotor-exit whirls and a corresponding increase in work output. As the turbine-exit pressure was decreased to an over-all pressure ratio somewhere between 0.198 and 0.132 (approximately 0.173 from fig. 6), the minimum static pressure that could be obtained at the stator exit was established. This, then, limited the amount of whirl that could be obtained from the stator and corresponded to the condition indicated by the sharp break in the operating curve of

figure 6. As the turbine-exit pressure was decreased further, a system of oblique shocks passed through the rotor passages with a corresponding increase in rotor-exit whirl and, hence, an increase in work output. The maximum work output occurred when the turbine-exit pressure was decreased to the indicated over-all pressure ratio of 0.030.

Comparison with design. - As indicated previously, the design of the turbine included the assumption of no significant change in flow characteristics radially from hub to tip. However, the design variation in outer-wall static pressure was calculated including the radial variation in static pressure required to satisfy simple radial equilibrium within the flow passages. This design variation in outer-wall static pressure is compared in figure 7(b) with the experimental results. The variation obtained from the minimum over-all pressure ratio p_4/p_0' of figure 7(a) is repeated in figure 7(b) for comparison purposes. Very close agreement exists at all stations except at the rotor inlet, where the experimental pressure is seen to be considerably higher than design. However, as pointed out in the section TURBINE DESIGN, a sharp recess was cut in the outer housing between the stator and rotor blade rows to provide rotor blade running clearance (inset, fig. 3). This recess could cause a radially outward flow of the streamlines in this region that would contribute to the indicated rise in static pressure above design.

It is noted from figure 7(b) that the static pressures at the stator and rotor outlet are both slightly above their design values, and both would tend to reduce the work output below design because the exit whirls would be less than design. If the stator-outlet static pressure, which is limited by the flow conditions within the rotor, could be decreased below the minimum value obtained experimentally, a resultant increase in work output should be realized because of an increase in stator-exit whirl. One method of accomplishing this would be to modify the rotor flow passage. This modification and its effect on turbine performance are discussed in the section entitled Effect of Rotor Modification.

Momentum-Loss Considerations

It has previously been indicated that the design procedure provided an area allowance for boundary-layer growth in the rotor passage that was too small. This area allowance was based on the boundary-layer equations used in the design procedure.

In order to obtain an indication of the actual momentum-loss characteristic encountered as compared with that resulting from the design procedure, an experimental ratio of effective rotor momentum thickness to

mean camber length $\overline{\theta}_{tot}/l$ was calculated by assuming that the following experimental conditions existed:

(1) design flow conditions at the rotor inlet (station 2, fig. 1)

(2) design free-stream flow angle at the rotor exit before mixing (station 3, fig. 1)

(3) negligible rotor blade trailing-edge thickness

(4) the same ratio of three-dimensional to two-dimensional momentum thickness as was used in the design

These assumptions resulted in an experimental ratio of effective rotor momentum thickness to mean camber length $\overline{\theta}_{tot}/l$ of 0.0114, which is comparable in magnitude to the results obtained from six transonic turbines reported in reference 8 and three subsonic turbines reported in reference 9. Figure 8 shows the results of the reference turbines as the ratio of effective rotor momentum thickness to mean camber length $\overline{\theta}_{tot}/l$ plotted against design total surface diffusion parameter D_{tot}. The experimental point for the subject turbine is shown at a design total diffusion parameter of 0.27. Although the turbine was designed for zero suction-surface diffusion and a pressure-surface diffusion of 0.27, it is felt that the total diffusion was considerably higher than 0.27 because the rotor-exit velocity was less than design. Of major interest is the fact that the general level of $\overline{\theta}_{tot}/l$ is approximately the same for the subject turbine, the subsonic turbines, and the transonic turbines. Apparently, the selected parameters may be correlated as done by the correlation curve of figure 8 without regard to the Mach number level of each individual turbine.

The previous considerations lead to two important observations:

(1) The effect of Mach number level, if any, on the ratio of effective rotor momentum thickness to mean camber length is small.

(2) The design procedure for a turbine of this type would be improved by calculating losses based on an assumed value of $\overline{\theta}_{tot}/l$, rather than basing the losses on the boundary-layer equations that were used in this design.

Effect of Rotor Modification

A large portion of the suction surface of the rotor blades was removed in an effort to decrease the minimum static pressure that could be

felt at the stator exit. This removal of metal from the suction surface in effect produced a free-streamline passage through the rotor. As pointed out in reference 2, one of the advantages of a free-streamline passage is that the effect of a change in turbine-exit pressure can propagate itself upstream through the rotor passage even though the velocities relative to the rotor are supersonic. A sketch of the amount of surface removed is shown in figure 9.

The effect of the rotor modification on turbine performance at design speed is shown in figure 10. The data points at design speed from the basic turbine performance curves of figure 6 are repeated in figure 10 for comparison with the results of the modified rotors. It can be seen from the figure that a slight improvement in performance was obtained. At design over-all pressure ratio, the improvement in specific work output amounted to about 3 percent.

Figure 11 shows the effect of the rotor passage modification on outer-wall static pressure. It can be seen from the figure that the attempt to lower the minimum stator-outlet pressure was successful. However, in so doing, the minimum static pressure that could be obtained at the rotor exit was increased because of a detrimental change in the flow pattern within the rotor that resulted in higher rotor losses. This, in turn, would tend to decrease the maximum work output. The net effect of the two counteracting tendencies was the slight improvement previously discussed.

In view of the fact that the over-all turbine performance was slightly improved by removing a large portion of the original suction surface of the rotor blades, the inference might be made that a detailed aerodynamic design of the rotor passage for such a turbine is unimportant. This is not so. The rotor losses of both the subject turbine and the cascade work of reference 2 increased when the blades were modified. It therefore appears that thorough aerodynamic design techniques are necessary to attain satisfactory rotor performance from supersonic turbines.

Supersonic Starting

The problems associated with supersonic starting of the rotor flow passages as described in reference 6 (cascade tests) were not encountered during the entire experimental investigation. The design procedure used for this turbine resulted in rotor passages that were critical in nature with respect to starting. In other words, the contraction of the flow passage at the rotor inlet was such that the passage could just start at the design entering relative Mach number of 2.0. In view of the fact that the stator produced slightly less than design whirl, the rotor entering relative Mach number must have been below the design value of 2.0.

This should have resulted in rotor passages that would not start supersonically. Apparently, the interaction of the flow between the stator exit and the rotor inlet was such that the normal shocks spanning the rotor inlet as described in reference 6 did not exist. This lack of both normal and strong oblique shocks can be noted from figure 8.

The stator throats were opened and closed to see if the starting problem could purposely be encountered. Also, the method of turbine operation at off-design conditions was varied in an attempt to set an unstarted rotor condition. However, the rotors started in every instance.

4931

SUMMARY OF RESULTS

The design and experimental investigation of a single-stage supersonic turbine are presented herein. The turbine was designed for a rotor entering relative Mach number of 2. The results of the investigation can be summarized as follows:

1. The equivalent specific work output obtained at design speed and approximately design over-all pressure ratio was 32.9 Btu per pound at a static efficiency of 0.414. This obtained static efficiency gave good verification to the theoretical results of an independent reference that predicted static efficiencies within the range 0.40 to 0.45 for single-stage turbines with similar design characteristics.

2. An experimental ratio of effective rotor momentum thickness to mean camber length was determined to be 0.0114. This compared favorably with the results obtained from several transonic and subsonic turbines, which indicates that the Mach number effect on this selected parameter is small.

3. The loss calculations based on the boundary-layer equations used in the design procedure resulted in a design-point static efficiency of 0.504. More area allowance for higher rotor losses should have been used with a resulting efficiency and work output at design conditions lowered to more reasonable values. This could be done during the design procedure by assuming a value of the ratio of effective rotor momentum thickness to mean camber length comparable to those determined to exist in transonic turbines.

4. The minimum static pressure that could be obtained at the stator exit was limited by flow conditions within the rotor. Removal of a large portion of the rotor suction surface enabled this minimum pressure at the stator exit to be reduced at the expense of higher rotor losses. The net effect was about a 3-percent improvement in turbine work output at design speed and design over-all pressure ratio.

5. No problems associated with supersonic starting were encountered during the entire investigation, even when the worst conditions of turbine operation with respect to this problem were imposed on the turbine. Apparently, the interaction of flow between the stator exit and rotor inlet was such that normal shocks or strong oblique shocks were not encountered. This was indicated by the static taps placed across the blade rows in the turbine outer housing.

Lewis Flight Propulsion Laboratory
National Advisory Committee for Aeronautics
Cleveland, Ohio, July 2, 1958

REFERENCES

1. Edelman, Gilbert M.: The Design, Development, and Testing of Two-Dimensional Sharp-Cornered Supersonic Nozzles. Rep. No. 22, M.I.T., May 1, 1948. (Bur. Ord. Contract NOrd 9661.)

2. Westphal, Willard R.: The Design and Cascade Tests of Free-Streamline and Full-Contour 160°-Turning Supersonic-Turbine-Blade Sections. NACA RM L57F21, 1957.

3. Stewart, Warner L.: Analytical Investigation of Multistage-Turbine Efficiency Characteristics in Terms of Work and Speed Requirements. NACA RM E57K22b, 1958.

4. Huppert, M. C., and MacGregor, Charles: Comparison Between Predicted and Observed Performance of Gas-Turbine Stator Designed for Free-Vortex Flow. NACA TN 1810, 1949.

5. Whitney, Warren J., Stewart, Warner L., and Miser, James W.: Experimental Investigation of Turbine Stator-Blade-Outlet Boundary-Layer Characteristics and a Comparison with Theoretical Results. NACA RM E55K24, 1956.

6. Boxer, Emanuel, Sterrett, James R., and Wlodarski, John: Application of Supersonic Vortex-Flow Theory to the Design of Supersonic Impulse Compressor - or Turbine - Blade Sections. NACA RM L52B06, 1952.

7. Whitney, Warren J., and Wintucky, William T.: Experimental Investigation of a 7-Inch-Tip-Diameter Transonic Turbine. NACA RM E57J29, 1958.

8. Stewart, Warner L., Whitney, Warren J., and Miser, James W.: Use of Effective Momentum Thickness in Describing Turbine Rotor-Blade Losses. NACA RM E56B29, 1956.

9. Nusbaum, William J., and Wasserbauer, Charles A.: Experimental Investigation of a High Subsonic Mach Number Turbine Having a 32-Blade Rotor with a Low Suction-Surface Diffusion. NACA RM E58F20, 1958.

TABLE I. - STATOR BLADE MEAN SECTION

COORDINATES

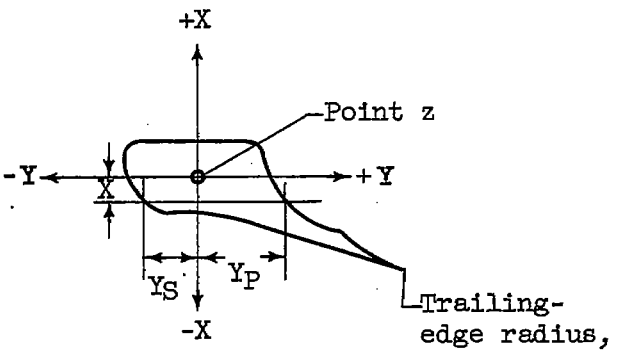

X, in.	Y_S, in.	Y_P, in.
0.200	-0.299	0.273
.150	-.387	.361
.100	-.400	.374
.050	-.395	.378
0	-.385	.387
-.050	-.364	.405
-.100	-.326	.436
-.150	-.264	.486
-.189	-.044	----
-.193	-.168	----
-.250	.323	.671
-.298	-----	.816
-.300	.488	.818
-.350	.647	.884
-.400	.812	.960
-.450	.978	1.048
-.483	----	1.122
-.487	1.125	1.125
-.492	1.120	-----

TABLE II. - ROTOR BLADE SECTION COORDINATES

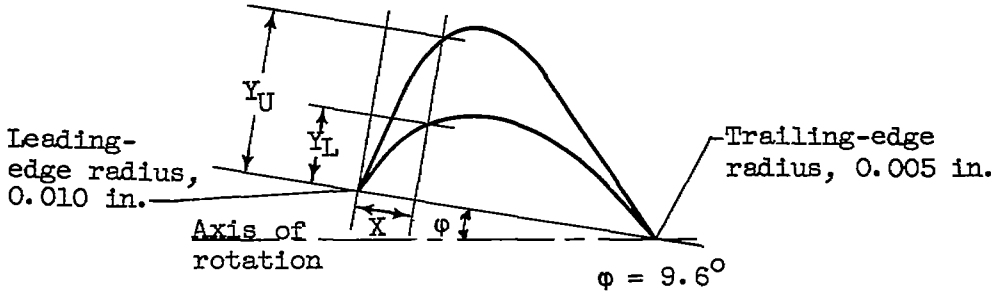

X, in.	Y_L, in.	Y_U, in.
0	0.010	0.010
.100	.193	.502
.200	.350	.830
.300	.444	.951
.400	.503	1.002
.500	.537	1.020
.600	.550	1.010
.700	.543	.967
.800	.521	.885
.900	.488	.777
1.000	.442	.667
1.100	.388	.557
1.200	.324	.446
1.300	.253	.336
1.400	.172	.226
1.500	.083	.115
1.595	.005	.005

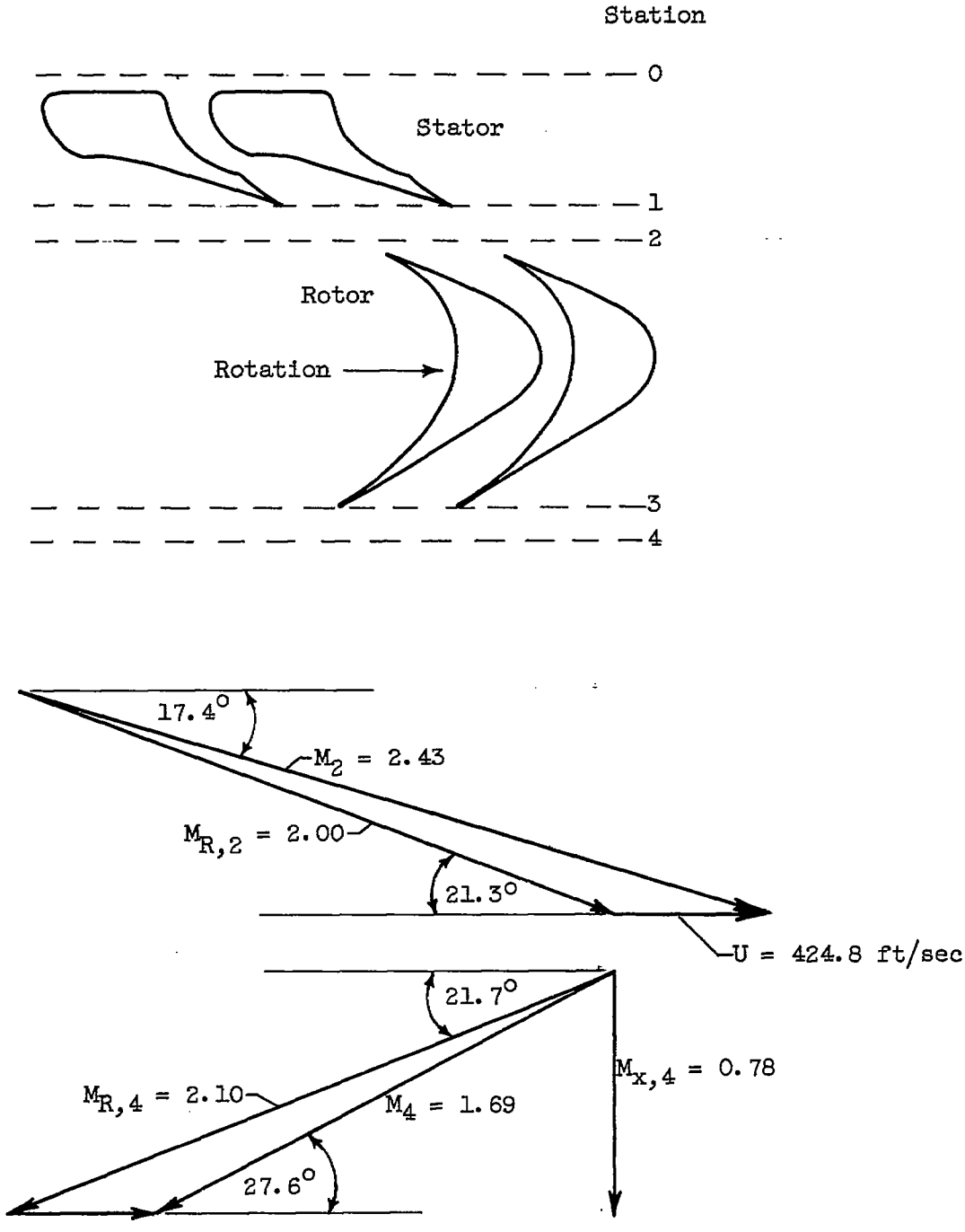

Figure 1. - Design after-mixing velocity diagrams.

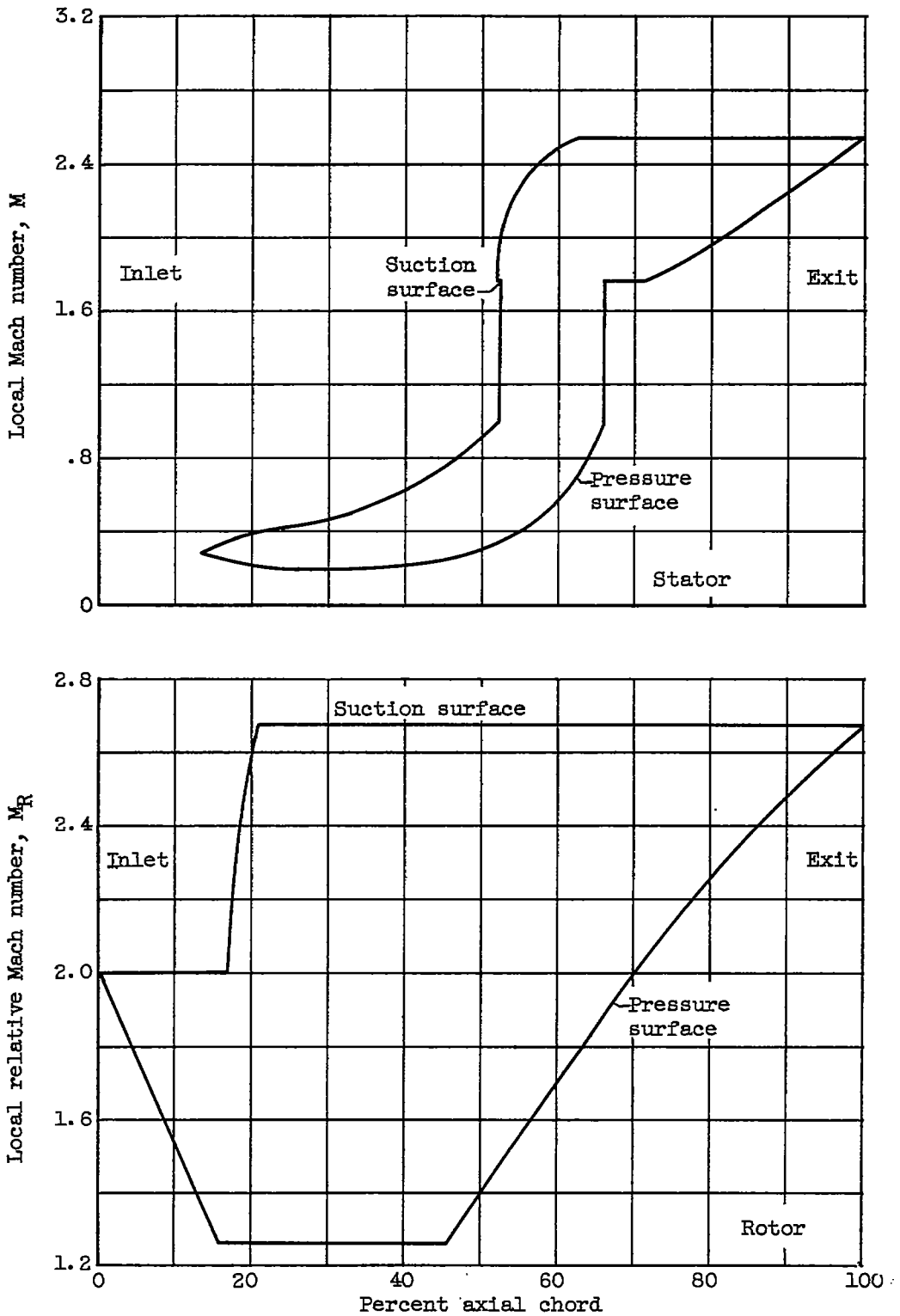

Figure 2. - Design blade surface velocities.

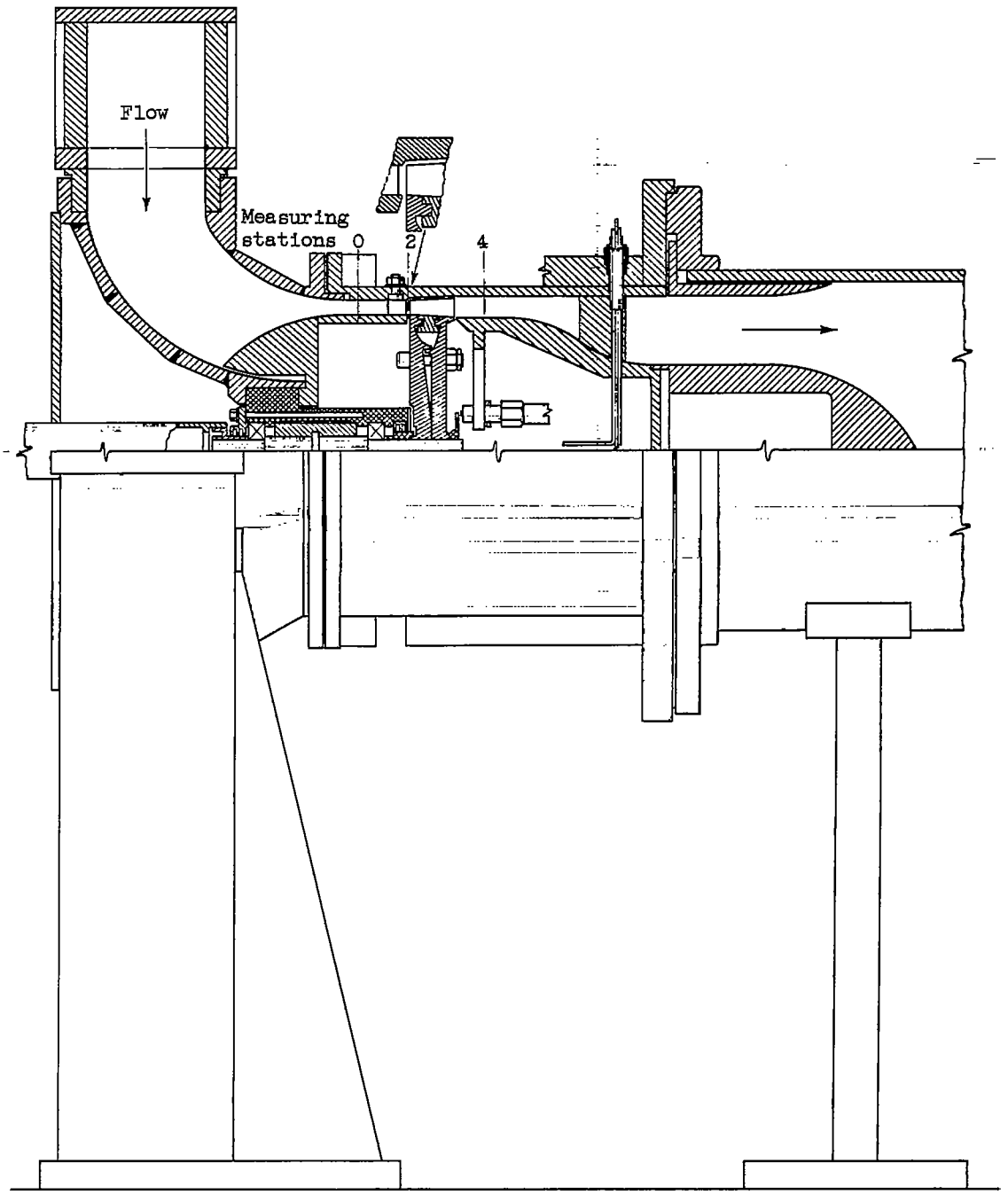

Figure 3. - Diagrammatic sketch of turbine test section.

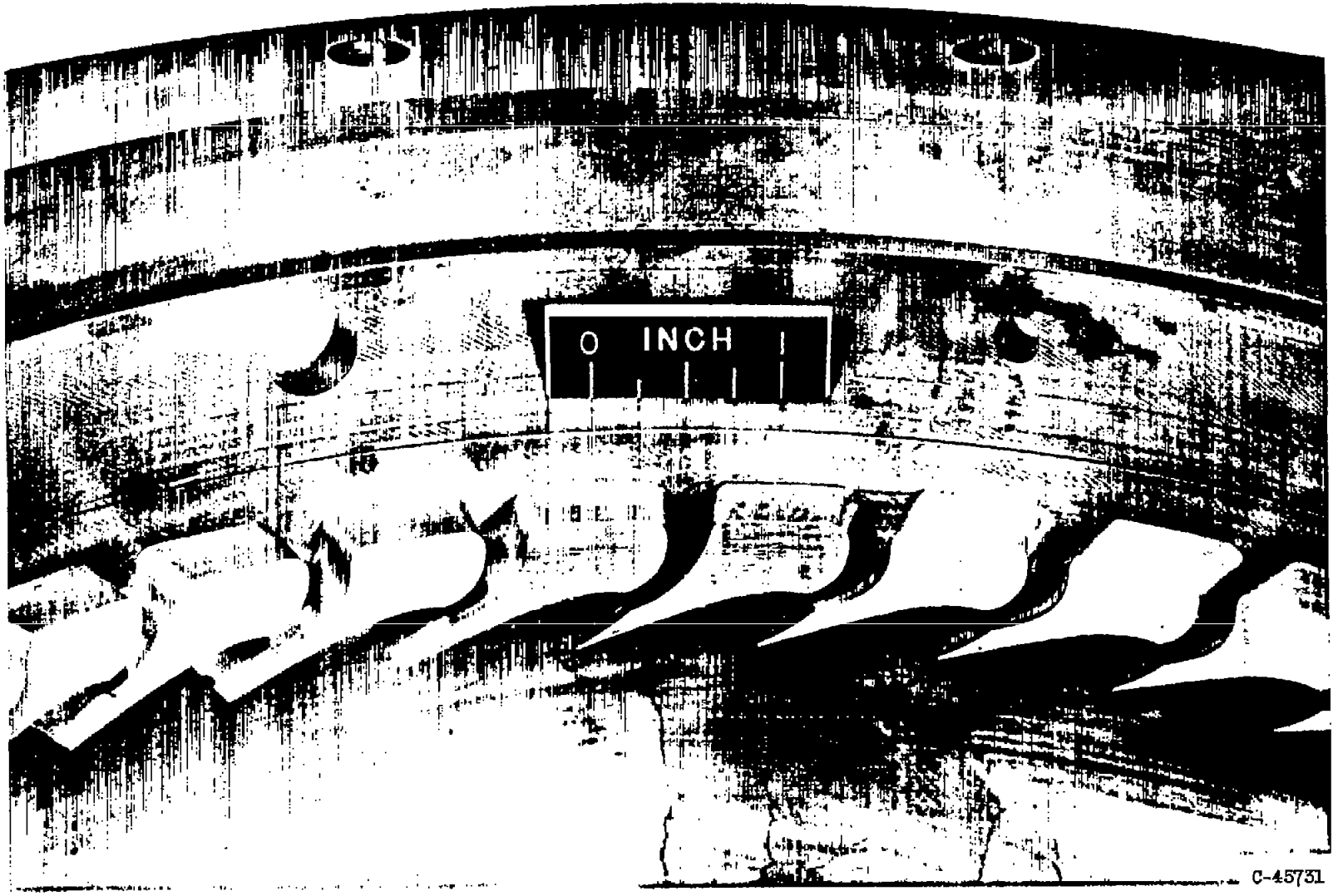

(a) Stator.

Figure 4. - Supersonic turbine blading.

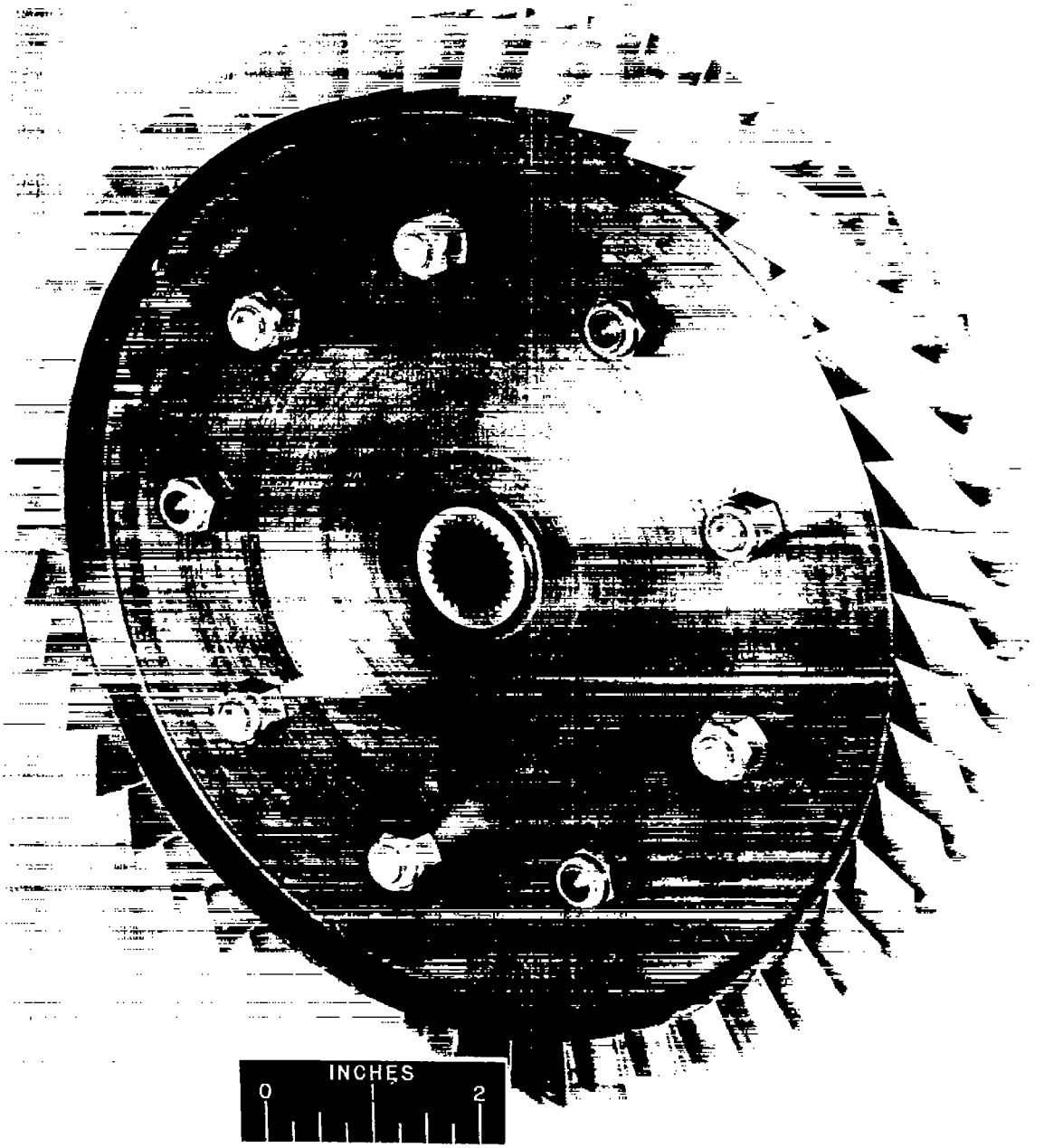

C-45730

(b) Rotor.

Figure 4. - Concluded. Supersonic turbine blading.

4931

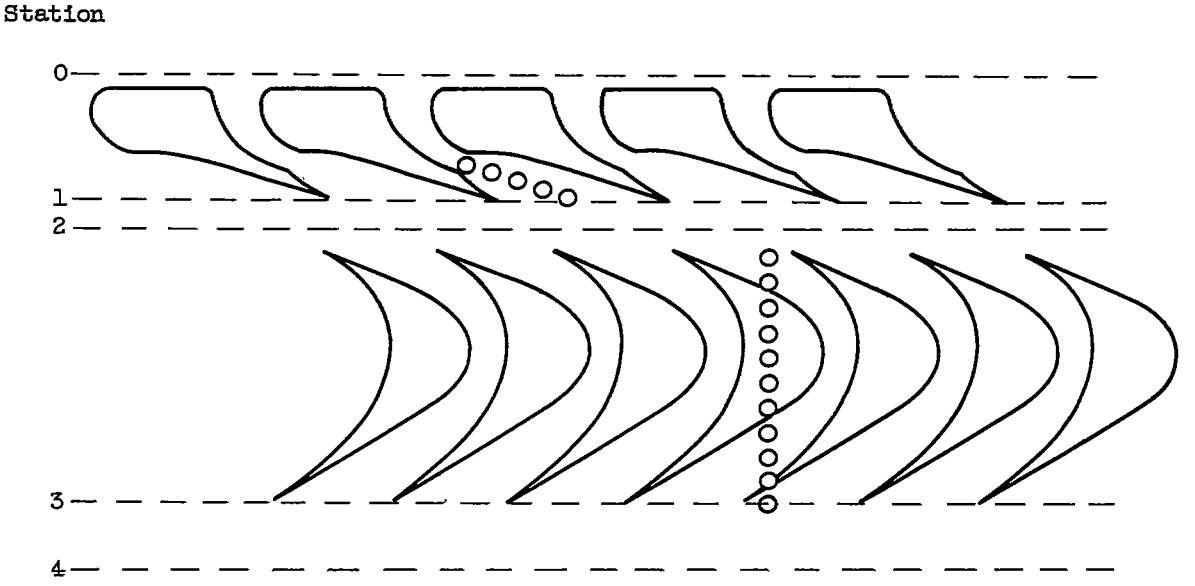

Figure 5. - Location of static-pressure taps on outer wall.

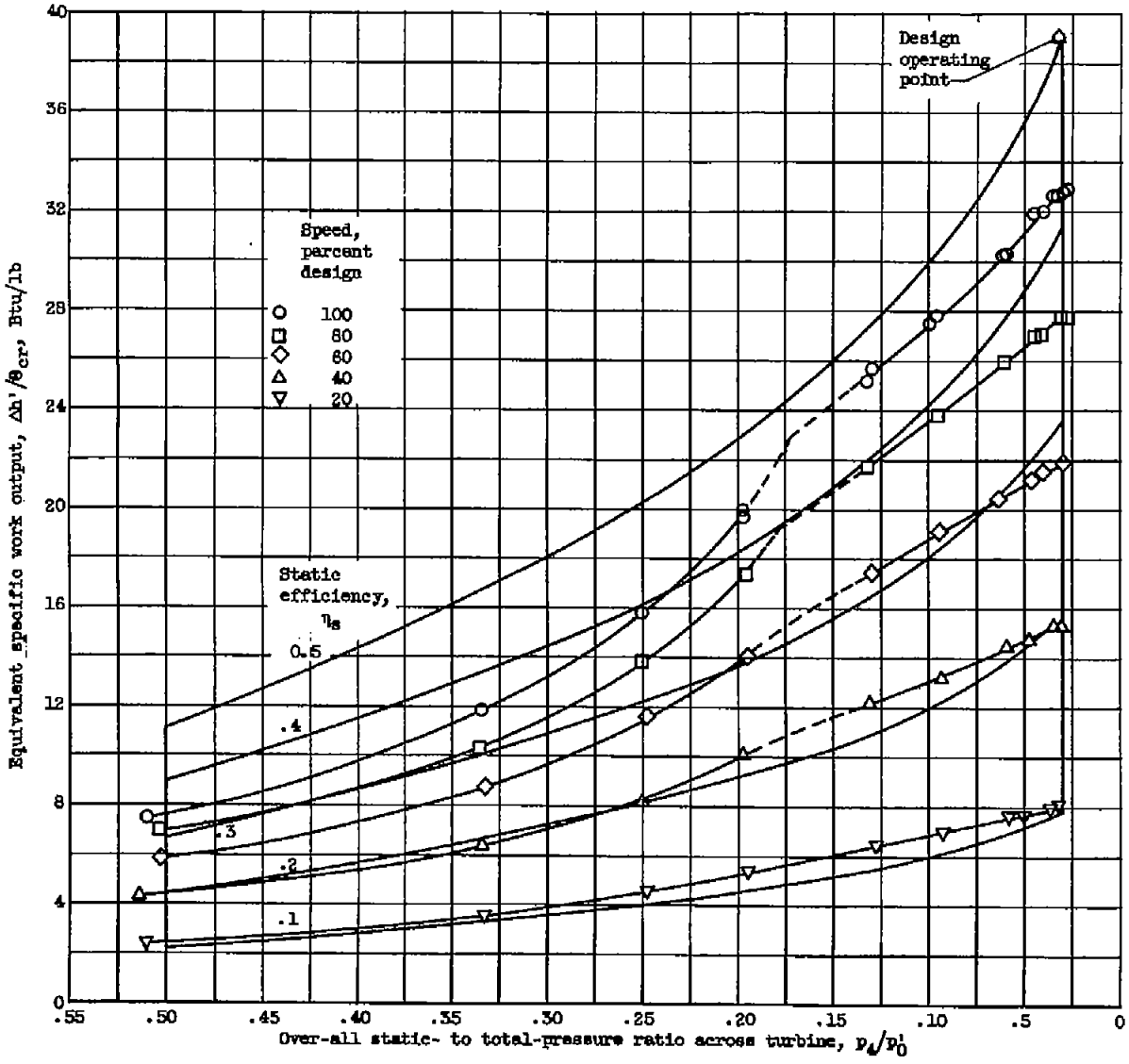

Figure 6. - Over-all turbine performance.

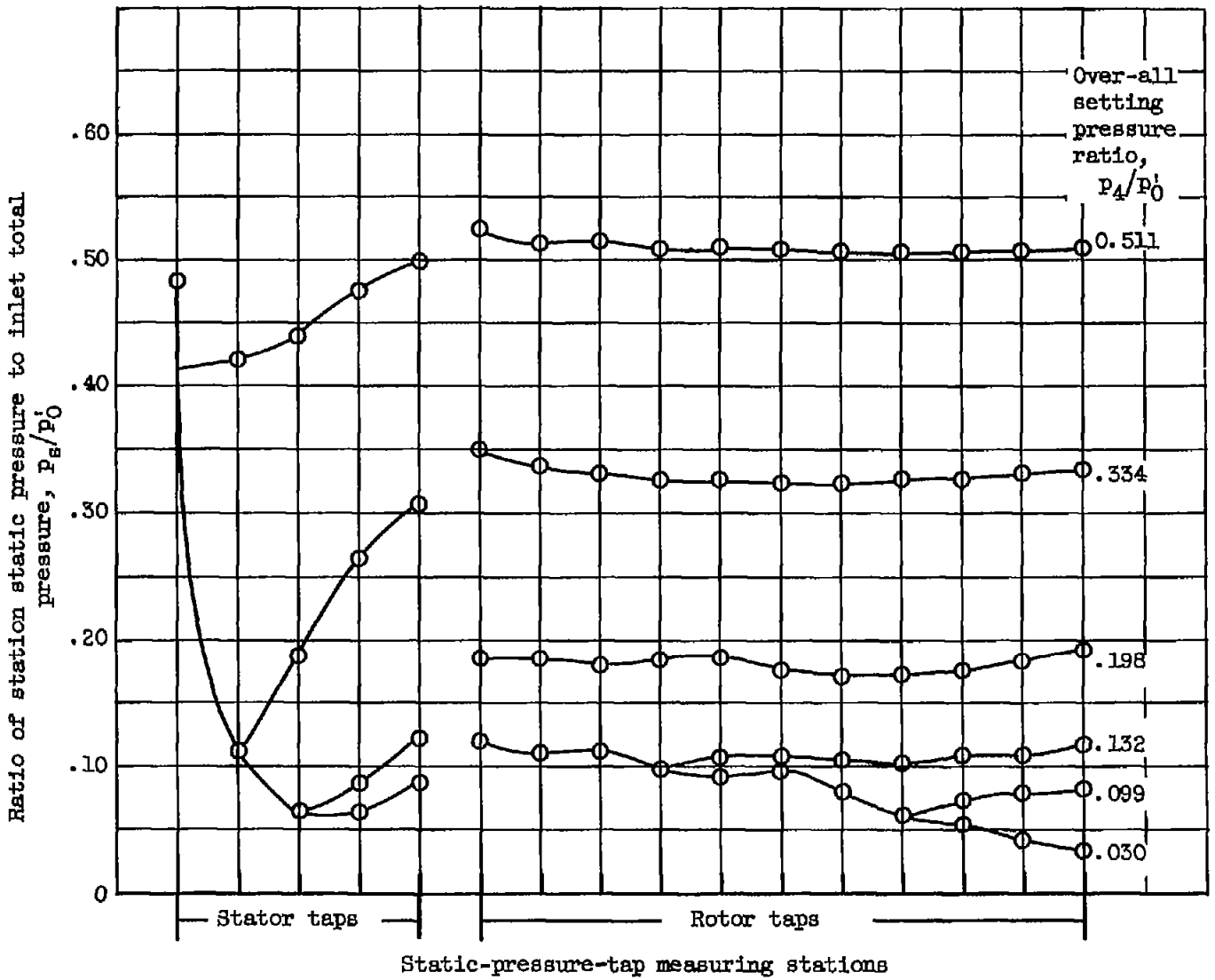

(a) Design speed.

Figure 7. - Outer-wall static-pressure variation.

(b) Correlation of experimental results with design.

Figure 7. - Concluded. Outer-wall static-pressure variation.

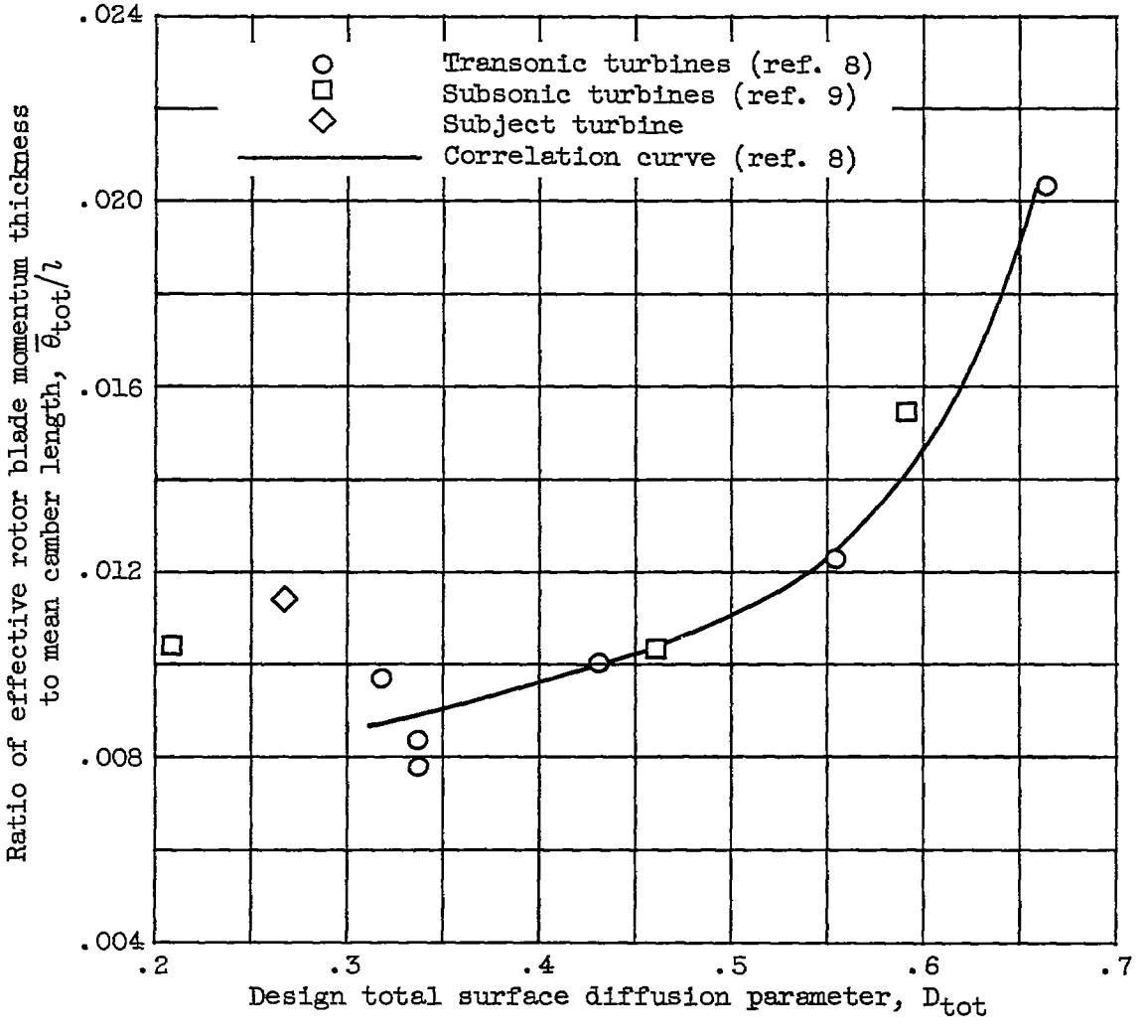

Figure 8. - Comparison of ratio of effective rotor blade momentum thickness to mean camber length of subject turbine with reference transonic and subsonic turbines.

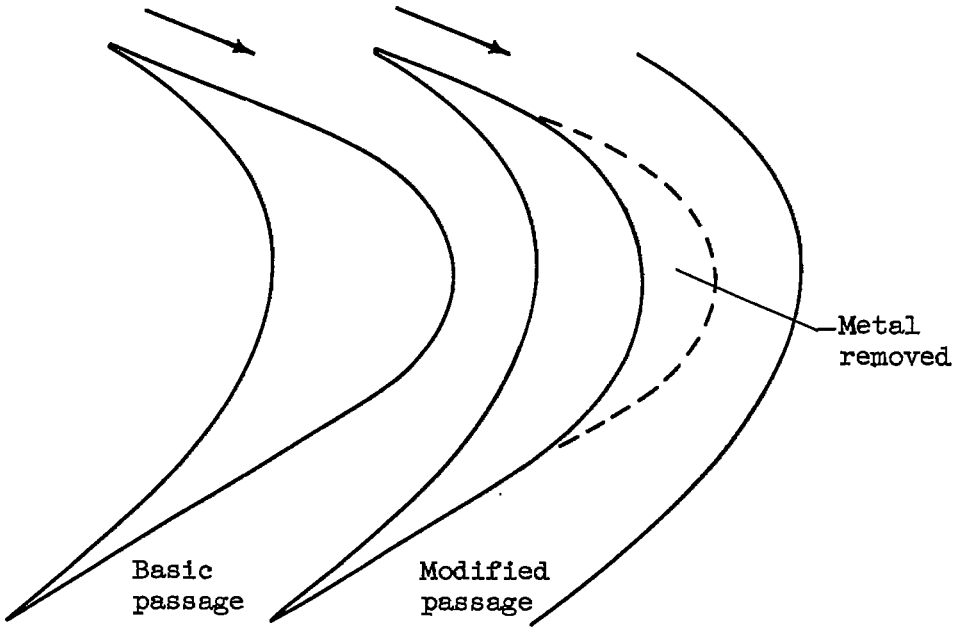

Figure 9. - Modification of rotor blade suction surface.

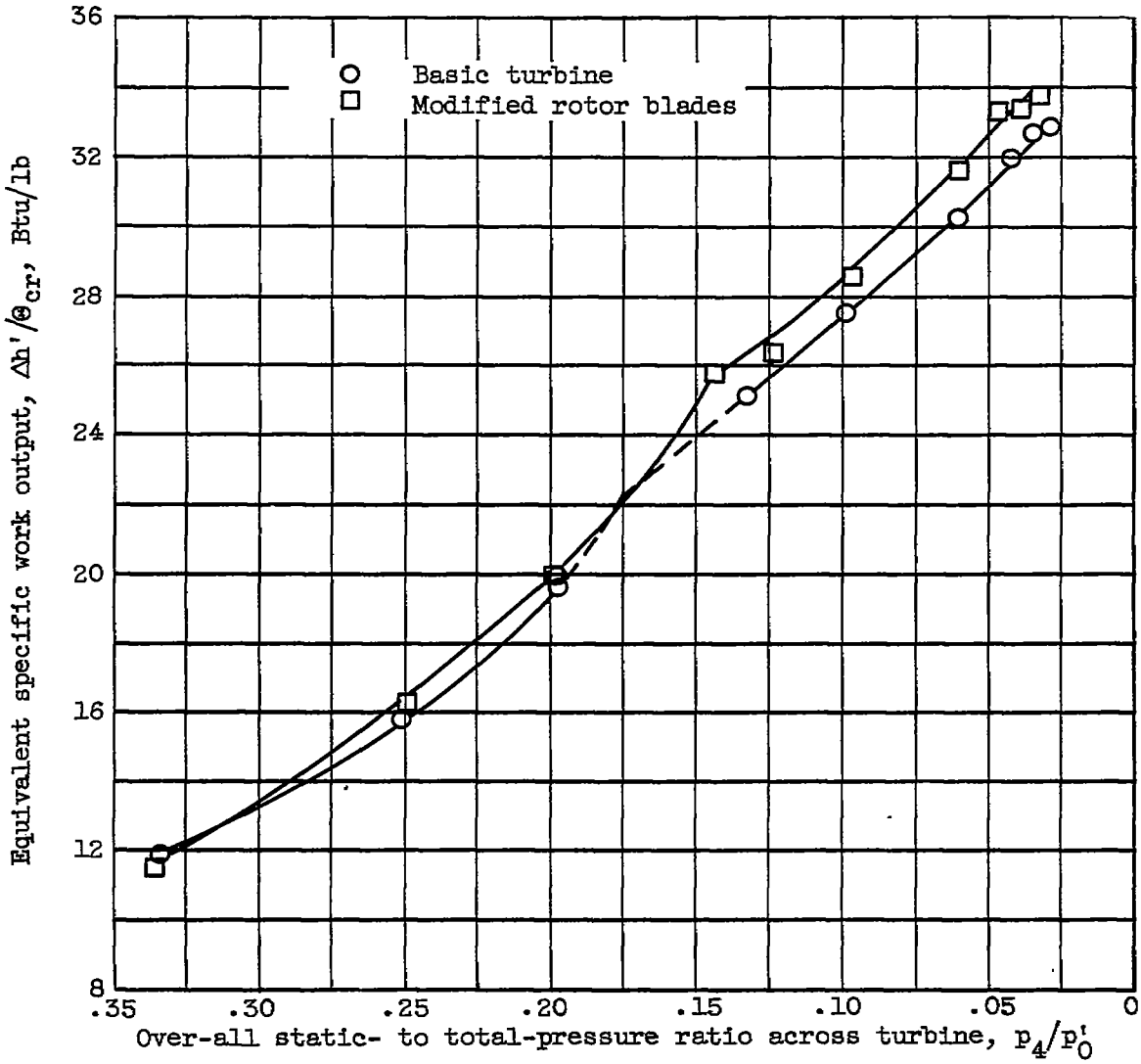

Figure 10. - Effect of rotor modification on turbine work output. Design speed.

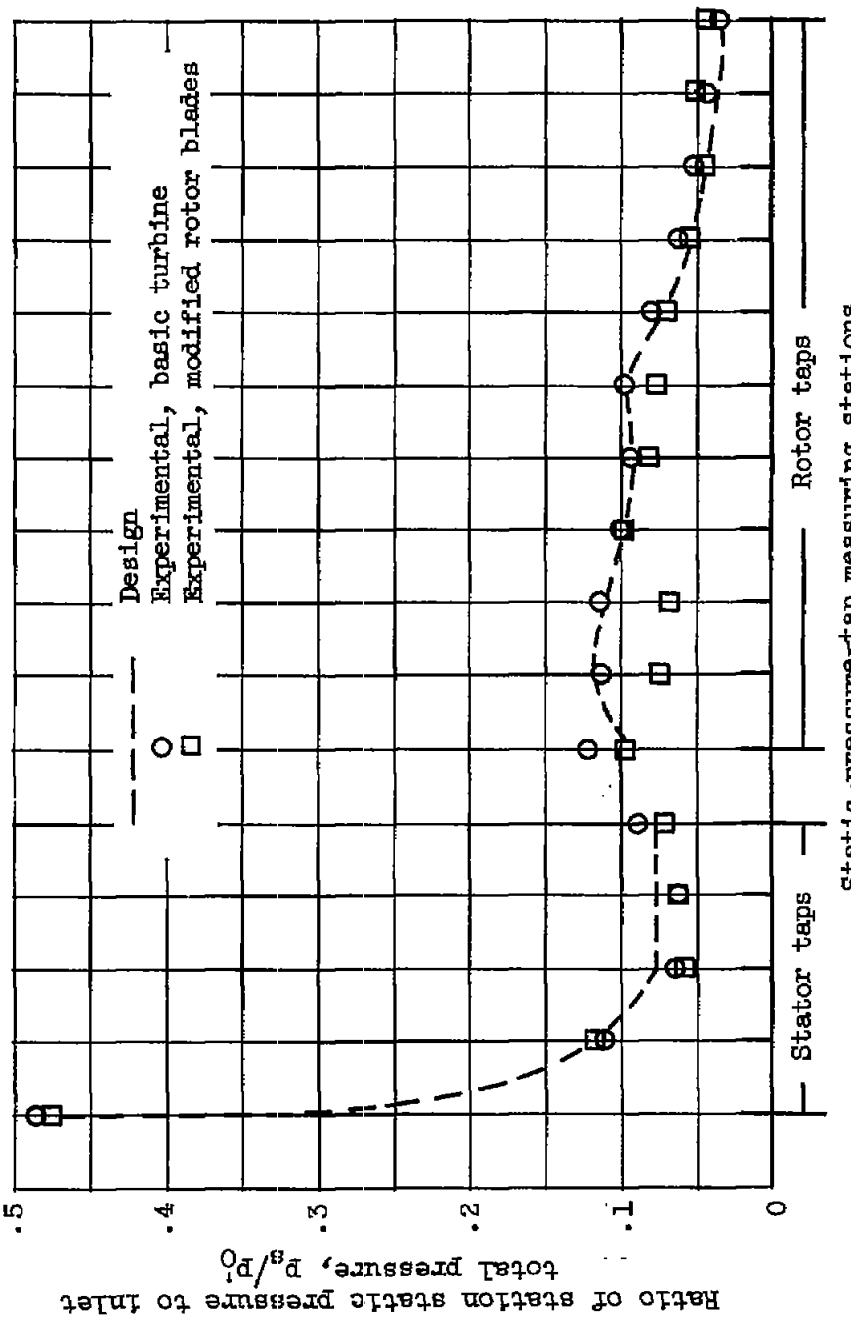

Figure 11. - Effect of rotor modification on outer-wall static-pressure variation.

NACA - Langley Field, Va.